

# RSC Advances



This is an *Accepted Manuscript*, which has been through the Royal Society of Chemistry peer review process and has been accepted for publication.

*Accepted Manuscripts* are published online shortly after acceptance, before technical editing, formatting and proof reading. Using this free service, authors can make their results available to the community, in citable form, before we publish the edited article. This *Accepted Manuscript* will be replaced by the edited, formatted and paginated article as soon as this is available.

You can find more information about *Accepted Manuscripts* in the [Information for Authors](#).

Please note that technical editing may introduce minor changes to the text and/or graphics, which may alter content. The journal's standard [Terms & Conditions](#) and the [Ethical guidelines](#) still apply. In no event shall the Royal Society of Chemistry be held responsible for any errors or omissions in this *Accepted Manuscript* or any consequences arising from the use of any information it contains.



Journal Name

ARTICLE

## Controlled Catalytic Domain Formation by Mixed Iron Halide Compounds to Decrease the Waviness of Carbon Nanotube Arrays

Received 00th January 20xx,  
Accepted 00th January 20xx

DOI: 10.1039/x0xx00000x

[www.rsc.org/](http://www.rsc.org/)

Sook Young Moon<sup>a</sup>

In this study, we present a method for controlling the waviness of carbon nanotube (CNT) arrays by adopting a two-phase catalytic system. In addition, we investigate the relationship between the catalyst state and the synthesis process of CNT arrays. As catalysts, we use two iron halides, iron(II) chloride and iron(III) chloride, combined in different ratios. The catalysts decompose and react with a silica surface on the substrate during the chemical vapor deposition process. The decomposed ions oxidize and precipitate over the substrate. An increased iron(III) contribution decreases the waviness of CNT arrays. Furthermore, we demonstrate that the catalyst state affects the alignment, diameter, length, and waviness of CNTs.

### Introduction

Carbon nanotubes (CNTs) have been considered for use in numerous applications because of their remarkable properties.<sup>1-5</sup> The development of CNTs as reinforcement material has attracted attention in composite science. However, some limitations of CNTs such as their poor dispersity in polymer matrixes, poor alignment, and short aspect ratio prevent their practical use. To overcome these limitations, many research groups have been developing well-aligned and high-aspect-ratio CNTs. Indeed, some groups have reported centimeter-scale CNT arrays. The composite materials prepared using these high-aspect-ratio CNTs exhibit high-volume fractions and enhanced mechanical properties. However, the size of these composites depends on the array size. This dependence is particularly important because large-scale, well-aligned CNT sheets are commercially demanded.

In 2002, Li et al. developed a spinnable CNT array.<sup>6</sup> The directly spinnable CNTs provide a promising approach to the development of high-performance CNT composites. Indeed, composites fabricated using directly spinnable CNTs exhibited drastically enhanced mechanical properties compared with those fabricated using powder-like CNTs.<sup>7-11</sup> Thus, many groups developed composites with a large aspect ratio and spinnable CNT arrays. However, the fabrication of composites with spinnable CNT arrays is difficult because of these arrays' limited availability. Only a few groups have achieved spinnable CNT arrays.<sup>12-14</sup> Thus, the process of fabricating highly spinnable CNT arrays is challenging.

Among the numerous factors that affect the synthesis of spinnable CNT arrays, the waviness of a CNT array is the most important because the dry-spinning process depends on the surface contact with neighboring CNTs to function through van der Waals forces. Consequently, the interactions between twisted CNTs are not sufficient for the spinning to occur because twisted CNTs cannot make surface contact with one another. Thus, CNT arrays should have a straight morphology. In addition, CNTs' spinnable fibers do not carry the load simultaneously and cannot be densely packed, thereby adversely affecting the properties of the resulting CNT composites, such as their strength, stiffness, and conductivity.

In this work, We have synthesized CNT arrays with controlled morphology by adopting a two-phase iron halide system. We studied the relationship between the catalyst chemical state and morphology of the CNT arrays, which affected their degree of spinnability.

### Experimental

**Fabrication of CNT arrays and sheets.** The CNT arrays were synthesized using a modified version of Inoue's method.<sup>15-16</sup> The CNT arrays were synthesized at 825 °C by a chemical vapor deposition (CVD) process in which acetylene (C<sub>2</sub>H<sub>2</sub>) was used as a carbon source. We used two types of iron(II/III) chloride with various compositions (xFeCl<sub>3</sub>:(1-x)FeCl<sub>2</sub>) as catalysts. Other conditions for the growth of CNT arrays were investigated, including various temperatures, gas ratios, and gas flow rates. To investigate the spinnability of the arrays, we fabricated super-aligned sheets using a spindle machine.

**Characterization.** The morphology of the synthesized CNT arrays was observed by field-emission scanning electron microscopy (FE-

<sup>a</sup> Structures and Advanced Composite Research Unit, Japan Aerospace Exploration Agency (JAXA), 6-13-1, Osawa, Mitaka, Tokyo 181-0015, Japan

† Footnotes relating to the title and/or authors should appear here.

Electronic Supplementary Information (ESI) available: SEM images of the substrate before the CVD process. See DOI: 10.1039/x0xx00000x.

SEM, Hitachi S-4700) and field-emission transmission electron microscopy (FE-TEM, JEOL 2100F, 200 kV). The spinnability of each CNT array was tested by directly pulling a CNT sheet away from the array using a spindle rotating system. The graphitic characteristics of the CNT arrays were analyzed by Raman spectroscopy (LabRAM HR Evolution, Horiba) under ambient conditions using a 523-nm YAG laser. The purity of the CNTs was determined by thermogravimetric analysis (TGA, TGA-6300; SII, Japan). The surface properties of the catalyst on the substrate were determined by X-ray photoelectron spectroscopy (XPS; Kratos Nova; Shimadzu, Japan).

## Results and discussion

Using two types of iron(II/III) halides combined in different ratios as  $[x\text{FeCl}_3:(1-x)\text{FeCl}_2]$ , we easily optimized the catalyst conditions for low-waviness CNT growth.

Figure 1 shows SEM images of the synthesized CNT arrays. The diameter of the synthesized CNTs ranged from 60 to 30 nm and their length varied from 1.2 mm to 600 nm, respectively. Both the diameter and length of the CNTs decreased as the values of  $x$  increased. The CNTs were straighter with increasing values of  $x$ . The waviness angle of the CNTs decreased from  $40^\circ$  to  $0^\circ$ .

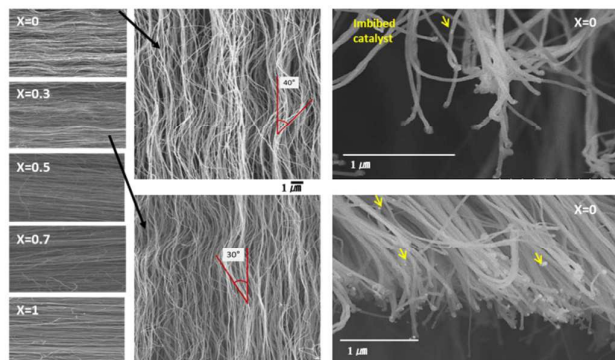


**Figure 1.** SEM images of the effect of catalyst composition  $[x\text{FeCl}_3:(1-x)\text{FeCl}_2]$ : (a),(f)  $x = 0$ ; (b),(g)  $x = 0.3$ ; (c)  $x = 0.5$ ; (d)  $x = 0.7$ ; and (e)  $x = 1$ .

Among numerous factors that affect waviness, catalyst imbibition inside the CNTs is a significant cause of defects. Specifically, it results in defects in the graphene layers. When the catalyst imbibition ceased, some graphene layers closed while other graphene sheets grew continuously. These halted catalyst points resulted in the curling of the CNTs (Figure 2), which explains the catalyst degradation during the CVD process. The catalyst particles also existed on the root of the CNT detached from substrate, producing only very weak adhesion strength on the substrate. Consequently, the catalysts are well imbibed into the inner part of the CNTs. Thus, increasing catalyst reactivity and/or adhesive strength on the substrate is very important for fabricating high-quality CNTs. Increasing the values of  $x$  resulted in a straight CNT

morphology, meaning that the catalyst was not present in the middle inner spaces. These results indicate that CNTs with low- or no-defect graphene structures are grown in the presence of  $\text{FeCl}_3$ , as also confirmed by the TGA results. After combustion in air, the residual amount decreased from 10% to 1% as the values of  $x$  increased.

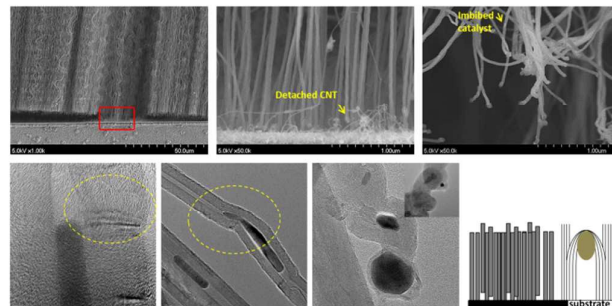


**Figure 2.** TEM images of the synthesized CNTs.

Raman spectroscopy is a nondestructive technique suitable for the structural and electrical characterization of CNTs. All the Raman spectra show two primary Raman bands at approximately  $1350$  and  $1580\text{ cm}^{-1}$ ; these bands are characteristic of a disordered (D-band) and  $sp^2$ -hybridized (G-band) carbon material, respectively (Figure 3). In general, the G-band indicates the presence of highly crystalline graphitic layers, whereas the D-band indicates the existence of defects in the graphitic layer.<sup>17</sup> Therefore, the integrated intensity ratio between the G-band and D-band ( $I_G/I_D$ ) is a measure of the crystallinity of carbon materials.

The  $I_G/I_D$  ratio was the largest for the CNTs grown with  $x = 1$ , which indicates that these CNTs are of higher quality compared to the other samples. Indeed, the  $I_G/I_D$  ratio increased from 2.0 to 2.8 with the values of  $x$ . The  $I_G/I_D$  ratio exhibited a strong correlation with the degree of waviness; the Raman spectra of the well-aligned regions exhibited a high  $I_G/I_D$  ratio, whereas the spectra of the wavy regions exhibited a low  $I_G/I_D$  ratio. These results indicate that the wavy regions contain more defects than the well-aligned regions and that the waviness is an intrinsic characteristic of individual CNTs. In particular, the appearance of a peak at approximately  $1617\text{ cm}^{-1}$  (the  $D'$  peak) indicates increased disorder.<sup>18</sup> Compared with the  $D'$  peak intensity for CNTs grown using the  $x = 1$  catalyst, that of the sample prepared using the  $x = 0$  catalyst was greater. This result is in exact accordance with the aforementioned considerations.

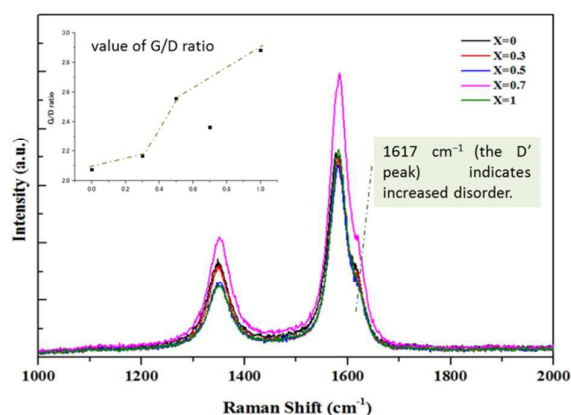


**Figure 3.** Raman spectra of CNTs prepared using  $[x\text{FeCl}_3:(1-x)\text{FeCl}_2]$  catalysts with various values of  $x$  (inset: change of the  $I_G/I_D$  ratio, where  $I_G$  and  $I_D$  represent the intensities of the G- and D-band, respectively).

The size and density of the catalysts determine the properties of the resulting CNTs, including their diameter, length, and crystallinity, as well as the density of their arrays. Therefore, we investigated the size and distribution of the catalyst particles on the substrate by annealing the CVD reaction at 825 °C to confirm the effect on the catalyst chemical state. The grain size of the iron particles of the  $\text{FeCl}_3$  over the substrate was smaller than the grain size of the iron particles of  $\text{FeCl}_2$  (Figure S1). The grain size at  $x = 0.5$  exhibited greater variation than the particles prepared using single components, which means that variation of the catalyst's composition can be used to control its distribution density and the particle size. The two iron halides have different melting points: 306 °C for  $\text{FeCl}_3$  and 677 °C for  $\text{FeCl}_2$ . Consequently, as the temperature increases, precipitation occurs twice. Therefore, the catalyst morphology changed compared with that obtained when only one type of iron chloride was used, as shown in the laser microscopy images (Figure S1).

In addition, the chemical reactivity between the active metal and the oxide support layers also affects the particle size distribution and adhesive strength of the catalyst on the substrate.<sup>19</sup> Ding et al.<sup>20</sup> have reported that iron ions are highly reactive and impregnate toward  $\text{SiO}_2$ -based support materials under a reducing atmosphere. In our experiments, the iron compounds also decomposed and reacted with the silica surface on the substrate during the CVD process. The decomposed ions oxidized and precipitated over the substrate, resulting in numerous etched pits. The iron ions with different charge states should exhibit different kinetic energies; thus, highly charged iron ions should be quickly reduced and should form metallic iron and/or iron oxide compounds. Consequently, increasing values of  $x$  resulted in a decreased number of etched pits on the  $\text{SiO}_2$  layer. Figure 4 shows the surface roughness of the substrate after the CVD process. This result is in exact accordance with the aforementioned considerations.

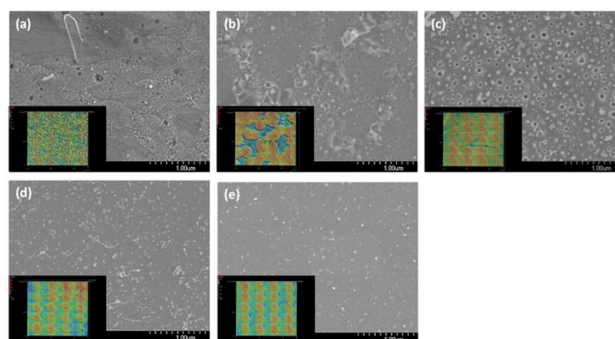


**Figure 4.** Laser microscopy images of substrates after CNTs were grown using  $[x\text{FeCl}_3:(1-x)\text{FeCl}_2]$  catalysts with various values of  $x$ : (a)  $x = 0$ , (b)  $x = 0.3$ , (c)  $x = 0.5$ , (d)  $x = 0.7$ , and (e)  $x = 1$ .

To investigate the catalyst state more specifically, we analyzed the substrate using XPS (Figure 5). The Fe 2p spectrum contained four dominant peaks: Fe 2p<sub>3/2</sub>, Fe 2p<sub>1/2</sub>, and their satellite peaks. The location of the 2p<sub>3/2</sub> peak varied between 709.6 and 711.1 eV depending on the catalyst composition. This shift of the binding-energy values can be interpreted in terms of the changing oxidation states of the iron or in terms of electron density. For  $x = 0$ , the Fe 2p peaks correspond to  $\text{Fe}_2\text{SiO}_4$  ( $\text{Fe}^{2+}$ ).  $\text{Fe}^{2+}$  ions react with  $\text{SiO}_2$  to produce an intermediate structure of fayalite ( $\text{Fe}_2\text{SiO}_4$ ). However,  $\text{Fe}^{3+}$  ions do not form this structure. With increasing values of  $x$ , the peak appears at 711.1 eV, which indicates that both  $\text{Fe}^{2+}$  and  $\text{Fe}^{3+}$  are present, likely in the form of  $\text{Fe}_3\text{O}_4$ ; a peak associated to Fe metal was also observed.

Teblum et al.<sup>21</sup> investigated the effects of iron oxide catalysts on the alignment of CNTs. They reported that the catalyst activity increased in the following order:  $\text{FeO} < \text{Fe}_2\text{O}_3 < \text{Fe}_3\text{O}_4 < \text{metallic Fe}$ . Consequently, metallic Fe exhibits the highest reactivity toward the synthesis of CNTs. In this work, the intensity of the metallic Fe peak increased with the values of  $x$ , indicating that the catalyst activity also increased with  $x$ . In general, the reduction of Fe occurs in the sequence  $\text{Fe}_2\text{O}_3 \rightarrow \text{Fe}_3\text{O}_4 \rightarrow \text{FeO} \rightarrow \text{Fe}$ . The Fe ions (2+/3+) reacted with  $\text{SiO}_2$  under the reducing atmosphere and were reduced to iron oxide and/or Fe(0) particles. These results were confirmed by the shifts and splitting of the peaks in the Si 2p and O 1s spectra (Figure S2).

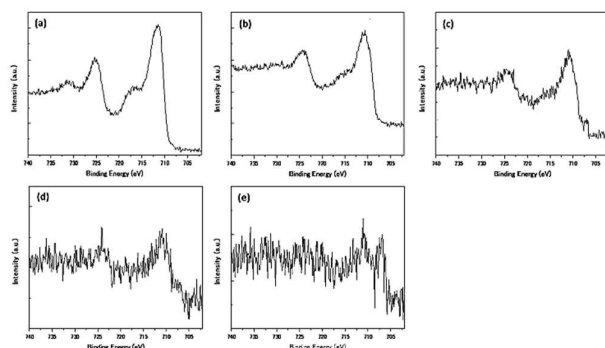


**Figure 5.** Fe 2p XPS spectra of substrates after CNTs were grown using  $[x\text{FeCl}_3:(1-x)\text{FeCl}_2]$  catalysts with various values of  $x$ : (a)  $x = 0$ , (b)  $x = 0.3$ , (c)  $x = 0.5$ , (d)  $x = 0.7$ , and (e)  $x = 1$ .

The synthesized CNT forests were used to fabricate super-aligned sheets using a spindle machine. As we explained before, the general mechanism of the spinning process is surface contact between CNTs by van der Waals forces. If an array had waviness, CNTs could not spin because of insufficient contact. Thus, CNTs should exhibit a straight morphology. As observed in our results, arrays with high values of  $x$  resulted in a straighter morphology such that they exhibited higher spinnability compared with arrays prepared using low values of  $x$  (Figure 6).

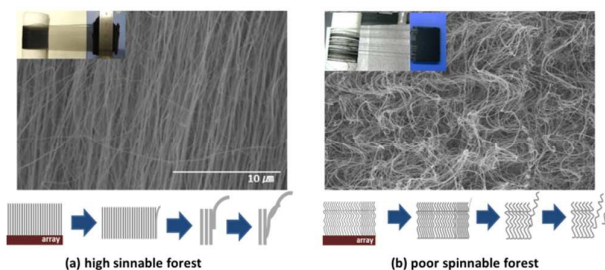


**Figure 6.** SEM images of the spinnable fibers responsible for the waviness of the CNT arrays: (a) straight arrays and (b) wavy arrays.

In addition, the preparation of well-aligned CNT sheets requires an appropriate density of CNTs on the substrate. Because the CNTs are too densely packed, they will release from the array in bundles, as shown in Figure 7a (Scheme 1).

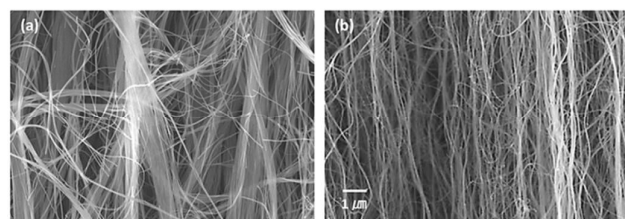
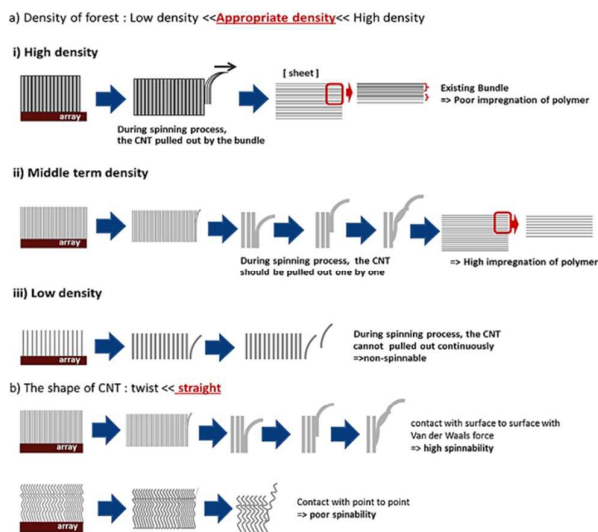


**Figure 7.** SEM images of CNT sheets forming (a) high-density and (b) intermediate-density forests.

Bundled CNTs exhibit increased strength; however, bundling is unfavorable to our purpose because it disturbs the impregnation of the polymer matrix during the preparation of composite materials. However, if the density of the CNT array is too low, the CNTs cannot spin because they cannot contact one another. Thus, the spacing between CNTs is an important factor that affects their spinning properties, as shown in Figure 7b. For these reasons, the CNT arrays should exhibit an appropriate density and a straight morphology to maximize the interactions among the CNTs. This relationship is illustrated in Scheme 1. Using two different catalyst compositions, we can easily control the density of the arrays.



**Scheme 1.** Proposed relationship between spinnability and CNT array conditions.

## Conclusions

We have developed a unique method for synthesizing spinnable CNT arrays by changing the catalyst's chemical state. We surmised that the catalyst's chemical state affected its reactivity, size, and distribution on the substrate. Consequently, the synthesized CNTs exhibited different diameters, lengths, densities, and waviness. The waviness of CNTs strongly affects their spinning properties. The CNT array with a straight alignment was highly spinnable; however, that with a wavy alignment was poorly spinnable. Thus, for the synthesis of spinnable CNT arrays, CNT arrays must be highly aligned without wavy regions. Moreover, an appropriate density of CNT arrays is desirable to prevent bundling during the spinning process. All these properties can be controlled via the catalyst state.

## Acknowledgements

The acknowledgements come at the end of an article after the conclusions and before the notes and references.

**Notes and references**

- 1 S. B. Sinnott and R. Andrews, *Crit. Rev. Solid State Mater. Sci.* 2001, 26, 145.
- 2 H. Dai, *Surf. Sci.* 2002, 500, 218.
- 3 R. H. Baughman, A. A. Zakhidov and W. A. de Heer, *Science* 2002, 297, 787.
- 4 M. Endo, T. Hayashi, Y. A. Kim and H. Muramatsu, *Jpn. J. Appl. Phys.* 2006, 45, 4883.
- 5 J. M. Schnorr and T. M. Swager, *Chem. Mater.* 2011, 23, 646.
- 6 Q. Li and S. Fan, *Nature* 2002, 419, 801.
- 7 T. Ogasawara, T. Tsuda and N. Takeda, *Compos. Sci. Technol.* 2011, 71, 73.
- 8 B. L. Wardle, D. S. Saito, E. J. Garcia, A. J. Hart, R. G. D. Villoria and E. A. Verploegen, *Adv. Mater.* 2008, 20, 2707.
- 9 T. Ogasawara, S. -Y. Moon, Y. Inoue, Y. Shimamura, *Compos. Sci. Technol.* 2011, 71, 1826.
- 10 T. Tsuda, T. Ogasawara, S. Y. Moon, K. Nakamoto, N. Takeda, Y. Shimamura and Y. Inoue, *Compos. Part A-Appl. S.* 2014, 67, 16.
- 11 T. Tsuda, T. Ogasawara, S. -Y. Moon, K. Nakamoto, N. Takeda, Y. Shimamura and Y. Inoue, *Compos. Sci. Technol.* 2013, 88, 48.
- 12 X. Lepro<sup>o</sup>, M. D. Lima and R. H. Baughman, *Carbon* 2010, 3621.
- 13 C. D. Tran, W. Humphries, S. M. Smith, C. Huynh and S. Lucas, *Carbon* 2009, 47, 2662.
- 14 C. P. Huynh, S. C. Hawkins, T. R. Gengenbach, W. Hymphries, M. Clenn and G. P. Simon, *Carbon* 2013, 62, 204.
- 15 Y. Inoue, K. Kakhata, Y. Hirono, T. Horie, A. Ishida and H. Mimura, *Appl. Phys. Lett.* 2008, 92, 213113.
- 16 Y. Inoue, Y. Suzuki, Y. Minami, J. Muramatsu, Y. Shimamura, K. Suzuki, A. Ghemes, M. Okada, S. Sakakibara, H. Mimura and K. Naito, *Carbon* 2011, 49, 2437.
- 17 A. Jorio, R. Saito, C. M. Lieber, M. Hunter, T. McClure, G. Dresselhaus and M. S. Dresselhaus, *Phys. Rev. Lett.* 2001, 86, 1118.; M. J. Matthews, M. A. Pimenta, G. Dresselhaus and M. S. Dresselhaus and M. Endo, *Phys. Rev. B* 1999, 59, R6585.
- 18 A. M. Rao, A. Jorio, M. A. Pimenta, M. S. S. Dantas, R. Saito, G. Dresselhaus and M. S. Dresselhaus, *Phys. Rev. Lett.* 2000, 84, 1820.
- 19 I. Sushumna and E. Ruckenstein, *J. Catal.* 1985, 94, 239.
- 20 X. Ding, M. F. Chiah, W. Y. Cheung, S. P. Wong, J. B. Xu, I. H. Wilson, H. Wang, L. Chen and X. Liu, *J. Appl. Phys.* 1999, 86, 2550.
- 21 E. Teblum, Y. Gofer, C. L. Pint and G. D. R. Nessim, *J. Phys. Chem. C* 2012, 116, 24522.